JASs Journal of Anthropological Sciences
Open Access
Research articles Vol. 104 (2026), pp. 1 - 15
doi. 10.4436/jass10408

Sexual dimorphism and body shape differences in hip bone morphology between *Homo sapiens* and Neanderthal lineage individuals

Gonzalo Madroñal-López[1,2], Nieves Candelas González[3,2], Armando González Martín[2], Markus Bastir[1] & Daniel García-Martínez[4,2]

1) Department of Paleobiology, Museo Nacional de Ciencias Naturales CSIC, Madrid, Spain
e-mail: gonzalo.mlopez@mncn.csic.es

2) Laboratorio de Poblaciones del Pasado (LAPP), Department of Biology, Faculty of Sciences, Universidad Autónoma de Madrid, Spain

3) Department of Prehistory, Ancient History and Archaeology, Faculty of Geography and History, Universidad Complutense de Madrid, Spain

4) Physical Anthropology Unit, Biodiversity, Ecology and Evolution Department, Universidad Complutense de Madrid, Madrid, Spain

Summary - *The pelvis as a whole and the hip bones are the best skeletal elements for determining sex in humans, as their pattern of sexual dimorphism is based on women's ability to give birth to a full-term fetus. Additionally, an individual's body type also has a significant effect on pelvic shape, which could, in turn, influence the pattern of sexual dimorphism. It has been demonstrated that 3D geometric morphometrics (3DGM) can distinguish between male and female hip bone morphology in anatomically modern humans. Therefore, this study employs 3DGM methodology to analyse and compare hip bone morphology of individuals from the Neanderthal lineage, as well as a specimen of early* Homo*, in a comparative framework of 46 H. sapiens of known sex. The Neanderthal lineage individuals were distributed along modern male and female morphologies, coinciding with their traditional sexual assessment, based on differences in pubic length, iliac width, and greater sciatic notch aperture. These results point to a similar coxal sexual dimorphism pattern in both lineages. Body shape does not seem to influence the dimorphic pattern, but the results show a gradient from archaic coxal morphology present in early Homo to the derived Neanderthal morphology, where the pre-Neanderthal individual has a more Neanderthal-like morphology than the* H. heidelbergensis *individual.*

Keywords - *Geometric morphometrics, Middle Pleistocene, Pelvis, Palaeoanthropology, Sex differences.*

Introduction

The pelvis as a whole and the hip bones individually are the best skeletal indicators of sex (Ferembach 1980; Klales 2020; Fischer et al. 2021). Their sexual dimorphism pattern is due to the unique ability of women to give birth to a full-term fetus, resulting in a wider internal cavity in female pelvises compared to male ones (Rosenberg 1992; Bruzek and Murail 2006; Rascón 2017). This pattern of sexual dimorphism is shared by all modern human populations (Betti 2014), and some researchers believe it appeared 100-150,000 years ago (Murail et al. 2005; Bruzek et al. 2017).

However, although the sex differences in the regions forming the pelvic canal are likely shared among primates and, by extension, were present in extinct hominin species (Fischer et al. 2021), the magnitude of sexual dimorphism varies between species, based mainly on differences in cephalo-pelvic proportions between the fetal head and pelvic canal size, as well as sexual size dimorphism and steroid hormone levels (Rmoutilová et al. 2024). The tight cephalo-pelvic proportions and

twisted birth canal shape present in *H. sapiens* make parturition in modern humans mechanically challenging and unique among the rest of primates (Rosenberg 1992; Franciscus 2009). However, it is still unclear when it appeared and whether other extinct hominin species had the exact same birth mechanism. The primitive nonrotational birth mechanism persisted at least until the Middle Pleistocene (Ruff 1995), but it is still debated whether Neanderthals had a modern-like rotational birth mechanism (Rosenberg 1992; Ponce de León et al. 2008) or a primitive nonrotational one (Franciscus 2009; Weaver and Hublin 2009). Regardless of their birth mechanism, their high encephalization quotients (Stanyon et al. 2003) made Neanderthal births difficult and required obligate midwifery (Franciscus 2009).

General body size and shape evolution in the genus *Homo* has been assessed through many different structures and measurements (pelvis, upper and lower limb length and proportions, femoral head breadth, thoracic height and width, etc.) and considering many different biological factors, like climatic variation, locomotion efficiency, or subsistence behaviour (Ruff 2002, 2010; Holliday 2012; Bastir et al. 2020). Carretero et al. (2004) identified three distinct body shapes: 1) the moderately tall, wide, and heavy archaic body shape characteristic of *Homo erectus*; 2) the short, wide, and heavy Neanderthal body shape, likely present in Middle Pleistocene hominins; and 3) the tall, narrow, and light modern body shape characteristic of modern humans. These changes in body shape have resulted in modifications to various anatomical regions, particularly the pelvis, leading to alterations in bi-iliac breadth and pubic length, among other characteristics (Arsuaga 1999; Carretero et al. 2004; Bonmatí et al. 2010), which, except for the superior pubic ramus length and the vertical position of the sacrum (Been et al. 2017), have little relation to the birth canal.

The pelvis is also involved in other functions like locomotion efficiency (Washburn 1960; Haeusler et al. 2021), thermoregulation (Auerbach 2018) and pelvic floor stability (Stansfield et al. 2021), which all influence pelvic morphology (Rmoutilová et al. 2024).

It has been demonstrated that 3D geometric morphometric (3DGM) techniques can differentiate size-independent male and female hip bone morphology in *Homo sapiens* (Bytheway and Ross 2010; Candelas et al. 2017; Robertson et al. 2019). 3DGM is a widely used tool in palaeoanthropological studies (Baab et al. 2012; López-Rey et al. 2025) and has been used to study hip bone morphology evolution (Betti et al. 2013; Lycett and von Cramon-Taubadel 2013) and pelvic sexual dimorphism through the inlet shape (Weaver and Hublin 2009; Fischer et al. 2021). Here we present the first application of these techniques to Neanderthal lineage individuals to compare their hip bone morphology with anatomically modern individuals. It could enable us to identify differences in the sexual dimorphism pattern between species and the possible influence that pelvic variations in body shape could have on sex differences, allowing us to test the following null hypotheses:

- H1: Neanderthal lineage individuals and *H. sapiens* have a similar sexual dimorphism pattern recognizable through geometric morphometrics techniques.
- H2: There are differences in hip bone morphology between the different body shapes, but they do not affect the sexual dimorphism pattern.

Material and methods

28 Type I and II landmarks were measured (Bookstein 1991) on regions with biological significance, especially those involved in the sexual dimorphism pattern following the proposal of Candelas et al. (2017) (Tab. 1, Fig. 1).

Sample

The sample consists of 46 *Homo sapiens* hip bones from the Almansa ossuary associated with the medieval Church of Santa María de la Soledad (Albacete, Spain, 13th-18th centuries; Candelas et

***Tab. 1** – Landmark descriptions (modified from **Candelas** et al. **2017**).*

LANDMARK	DESCRIPTION
1	Most prominent point of the anterior superior iliac spine
2	Most prominent point of the anterior inferior iliac spine
3	Union between the base of the anterior inferior iliac spine and margin of the acetabulum
4	Highest point on the iliac crest
5	Most prominent point of the posterior superior iliac spine
6	Most prominent point of the posterior inferior iliac spine
7	In dorsal view, the most salient point on the iliac tubercle towards the observer
8	In ventral view, the most salient point on the iliac crest towards the observer
9	Apex of the auricular surface of the ilium
10	Most anterior point over the end of the superior half of the auricular surface of the ilium
11	Most posterior point over the end of the superior half of the auricular surface of the ilium
12	Joint between base of the ischial spine and anterior end of the greater sciatic notch
13	Point of maximum curvature in the greater sciatic notch
14	Point on the arcuate line of the straight line that connects landmarks 4 and 18
15	Point on the arcuate line of the straight line that connects landmarks 1 and 18
16	Point on the arcuate line of the straight line that connects landmark 18 with the most salient end of the iliopubic eminence
17	Point on the arcuate line of the straight line that connects landmark 18 with the middle point of the base of the pubic tubercle
18	Most inferior point on the ischial tuberosity
19	Union between ischial tuberosity and ischiopubic ramus
20	Highest point of pubic symphyseal face
21	Lowest point of pubic symphyseal face
22	Midpoint of pubic symphyseal face
23	Projection of landmark 22 over the anterior rim of the obturator foramen
24	Acetabular point (Rissech et al. 2001)
25	Anterior end of the lunate surface in acetabular fossa
26	Posterior end of the lunate surface in acetabular fossa
27	Point on the acetabular rim of the straight line that connects landmarks 3 and 18
28	Central point of acetabulum into the acetabular fossa

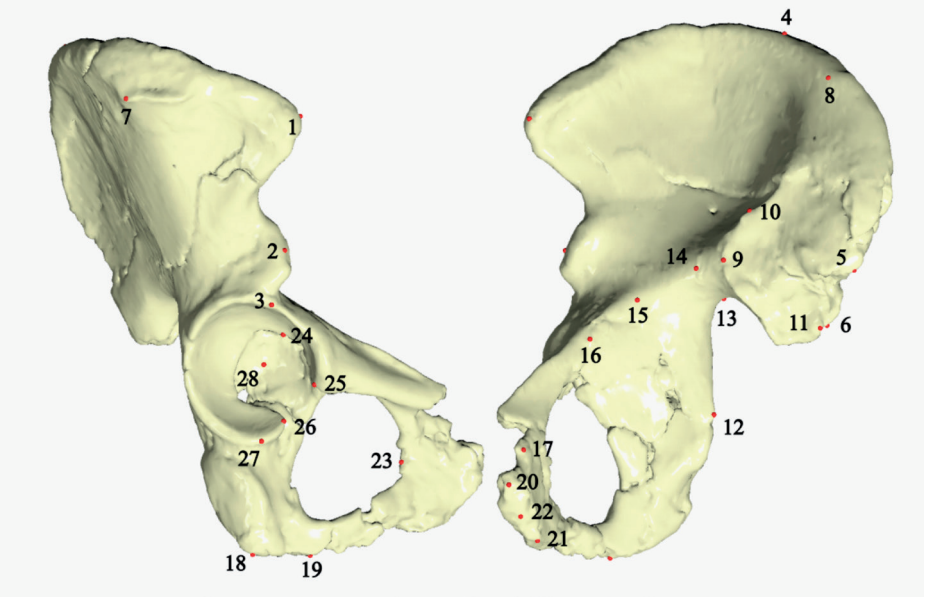

***Fig. 1** – Graphic representation of the selected landmarks on the Kebara 2 individual.*

al. 2017), and six fossil individuals, three from the Upper Pleistocene: Kebara 2 (Rak and Arensburg 1987), Tabun C1 (McCown and Keith 1939), and Feldhofer 1 (Schaaffhausen 1888), two from the Middle Pleistocene: the left hip bone of SH Pelvis 1 (Arsuaga et al. 1999) and Arago XLIV (de Lumley 2015), and the Lower Pleistocene individual KNM-ER 3228 (Leakey 1976) (Tab. 2). We divided the sample into two analyses. We used all the fossils for an exploratory analysis of body shape, using the early *Homo* individual as an outgroup (the archaic body shape in Carretero et al. 2004). We then removed the KNM-ER 3228 individual from the sample to perform the sexual dimorphism analyses to remove the noise of the archaic individual with, expectedly, a different sexual dimorphism pattern.

Methodology

For the anatomically modern individuals, the landmarks were digitized using the MicroScribe G2 tool (Immersion Corp., San Jose, CA, USA). The fossil individuals were measured on 3D digital models using the Viewbox 4 software (4.1.0.12 BETA version, dHAL Software, Kifissia, Greece). The Kebara 2 model was obtained from a CT scan and is part of the collection of virtual anthropology of the Museo Nacional de Ciencias Naturales (MNCN- CSIC). The Feldhofer Grotte 1 model was obtained from a surface scan of a research quality cast, and is part of the collection of the Research Laboratories of Archaeology of the University of North Carolina, available at Sketchfab (https://sketchfab.com/3d-models/homo-neanderthalensis-neanderthal-1-433rp10-747c435d906342e8a492c93e1e00aa57). The 3D model used for Tabun C1 is the reconstruction made by Weaver and Hublin (2009) from a micro-CT scan of the original fossil. High resolution 3D models were made for the rest of the sample using an Artec Spider scanner (Bastir et al. 2019). The Arago XLIV model was obtained from a research quality cast and the KNM-ER 3228 model from the original fossil, both housed in the National Museums of Kenya. The SH Pelvis 1 model was obtained from a research quality cast housed in the Museo Arqueológico Nacional in Madrid. All permissions to access and use the sample were granted.

***Tab. 2** – Hominid fossils used in the study.*

SPECIMEN	TAXONOMY	CHRONOLOGY	GEOGRAPHY	SEXUAL ASSESSMENT
Kebara 2	*H. neanderthalensis*	Upper Pleistocene	Levantine	Male
Tabun C1	*H. neanderthalensis*	Upper Pleistocene	Levantine	Female
Arago XLIV	Late pre-Neanderthal	Middle Pleistocene	European	Female
SH Pelvis 1	Early pre-Neanderthal	Middle Pleistocene	European	Male
Feldhofer 1	*H. neanderthalensis*	Upper Pleistocene	European	Male
KNM-ER 3328	Early *Homo*	Lower Pleistocene	African	Male

For the comparative human sample, we used 25 male and 21 female individuals, whose sex was determined by previous researchers (Candelas et al. 2017) using the DSP method (Murail et al. 2005). As for the fossil sample, Kebara 2, SH Pelvis 1, and KNM-ER 3228 were initially assessed to be male (Rak and Arensburg 1987; Arsuaga et al. 1999; Leakey 1976), while Tabun C1 and Arago XLIV were assessed as females (McCown and Keith 1939; de Lumley 2015). Feldhofer 1 has been genetically confirmed to be male (Skoglund et al. 2013).

The Almansa individuals were selected because of their remarkable state of preservation, but the fossil individuals are highly fragmented. The missing landmarks were digitized through geometric reconstruction, which is based on the properties of thin-plate spline interpolation (Gunz et al. 2009). Kebara 2 was used as the reference, as it was the only fossil individual that preserved the 28 landmarks. This reconstruction method may introduce bias in the results, making the estimated morphology of the individuals more similar to the reference morphology (Kebara 2: male, Upper Pleistocene) than it would be in the complete fossil. To minimize this bias, two more reconstructions were made for each individual using the reconstructed SH Pelvis 1 (male, Middle Pleistocene) and Tabun C1 (female, Upper Pleistocene) as references. The final sample consists of 60 individuals: 46 *Homo sapiens* and 14 fossil individuals.

All landmark configurations were centered, scaled, and rotated using a Generalised Procrustes Analysis (Zelditch et al. 2012), and the resulting Procrustes shape coordinates were used to perform a Principal Component Analysis (PCA). Size differences were analysed using the centroid sizes (CS). A Kolmogorov-Smirnov (K-S) test was performed to assess normality, and a Welch t-test was used to compare sizes between groups. To test the classification performance across groups, a PCA was performed using only the extant human individuals, and a Linear Discriminant Analysis (LDA) model was trained using the DSP sexual classification and the *H. sapiens* Principal Component (PC) 1 scores. Then, the Neanderthal lineage individuals were introduced into the *H. sapiens* morphospace, using the modern mean shape as the reference to centre the newly included individuals, and they were introduced into the LDA model. All statistical analyses were performed in RStudio v. 2025.09.2 (R Core Team 2025) using the packages 'geomorph' v. 4.0.10 (Baken et al 2021; Adams et al. 2025), 'ggplot2' v. 4.0.1 (Wickham 2016), 'Morpho' v. 2.13 (Schlager 2017), 'MASS' v. 7.3-65 (Venables and Ripley 2002), and 'stats' v. 4.5.2 (R Core Team 2025). To test the separation between groups, a Discriminant Function Analysis (DFA) based on a T-squared test was performed in the MorphoJ software (Klingenberg 2011). The 3D results were visualized using the EVAN Toolbox v. 1.75 (EVAN-Society 2010) software (Bastir et al. 2019).

Results

The CS of the 60 hip bones were normally distributed (K-S; p = 0.516), with the *H. sapiens* hip bones (mean CS = 359.846, std. dev. = 17.100) being smaller (p < 0.001) than the archaic individuals (mean CS = 391.555, std. dev. = 25.391), and also smaller (p = 0.001) than the Neanderthal lineage individuals (mean CS = 395.846, std. dev. 27.240).

For the whole sample PCA, PCs 1-3 account for 49.25% of the total variability; in the Neanderthal lineage PCA, PCs 1-3 account for 48.94%. The low variability explained by each principal component means that the variability depends on different regions of the bone, rather than on a single anatomical structure. We selected only the first three PCs for the analyses because they reflected the most relevant morphological and biologically meaningful features to assess the problem of this study, and also because they are the only ones that explain more than 10% of the variability and represent almost 50% of the total variance.

In both analyses, PC1 (26.89% for Neanderthal lineage data; 27.24% for the whole sample) divides the *H. sapiens* and extinct individuals. As seen in Figures 2 and 3, archaic individuals present longer pubic bones, pronounced lateral flaring of the iliac blades, a more concave arcuate line, and a laterally positioned acetabulum.

Sexual dimorphism

In the Neanderthal lineage PCA, sexual dimorphism is most clearly represented in PC3 (10.53%), but PC2 (11.52%) also contains differences typically associated with sexual dimorphism in the hip bones. Anatomically modern humans are clearly separated into male and female morphologies. Both groups were determined using 95% equal frequency ellipses (Fig. 4), where only two female and three male individuals remained in the intersection zone. There seems to be a diagonal gradient, where lower PC2 and PC3 values indicate a female morphology and higher values in both axes indicate a male shape. The female morphology is characterized by a relatively longer pubis and shorter ischium, a wider greater sciatic notch (GSN), a wider ilium, and a longer arcuate line. The Neanderthal lineage individuals are also grouped as male and female following the diagonal gradient. Kebara 2 is placed at the intersection level of the *H. sapiens* individuals, and the Arago XLIV placement in the morphospace is highly dependent on the reconstruction.

The differences between the mean shapes were statistically significant between the male and female *Homo sapiens* (Procrustes distance = 0.073, p < 0.001), between males (Procrustes distance = 0.145, p < 0.001) and females (Procrustes distance = 0.167, p < 0.001) from both lineages, modern males and Neanderthal lineage females (Procrustes distance = 0.176, p < 0.001), modern females and Neanderthal lineage males (Procrustes distance = 0.148, p < 0.001), and also between the "male" and "female" means of the individuals from the Neanderthal lineage (Procrustes distance = 0.117, p = 0.010).

The *H. sapiens* PCA's PC1 divides the individuals by male and female morphologies (Candelas et al. 2017). The LDA model classifies modern females with a 90.48% accuracy (19/21), and males with a 96% accuracy (24/25). Introducing the Neanderthal lineage individuals in the anatomically modern morphospace and projecting them onto the *H. sapiens* PC1 results in none of the fossil individuals being out of range, and four reconstructions were classified with less than 90% probability. Most of the fossil classifications match their traditional sexual assessment, with just two exceptions: Kebara 2 and Arago XLIV's reconstruction based on SH Pelvis 1 (Tab. 3).

Body shape influence

In the sample that includes the early *Homo* individual, body shape is most represented by PC2 (11.75%), but it also contains differences usually attributed to sexual dimorphism. The *H. sapiens* individuals do not show any clear pattern along the PC2 distribution (Fig. 2). Neanderthal individuals cluster together in the positive values except for Feldhofer's reconstruction using Pelvis 1 as the reference, which clusters with the Middle Pleistocene individuals. The positive values

***Tab. 3** – Linear Discriminant Analysis (LDA) results including PCA values, sexual classification and statistical probability of belonging to the group.*

SPECIMEN	PC1 VALUE	PREDICTED GROUP	PROBABILITY
Kebara	-0.017	Female	0.912
Arago XLIV_k2	-0.029	Female	0.989
Arago XLIV_SH	0.006	Male	0.856
Arago XLIV_t1	-0.044	Female	0.999
Feldhofer 1_k2	0.005	Male	0.848
Feldhofer 1_SH	0.024	Male	0.994
Feldhofer 1_t1	0.030	Male	0.998
Tabun C1_k2	-0.031	Female	0.992
Tabun C1_SH	-0.006	Female	0.584
SH Pelvis 1_k2	0.008	Male	0.901
SH Pelvis 1_t1	0.008	Male	0.899

describe a slightly narrower ilium with its highest point being in the medial part of the bone, a smaller and more laterally oriented acetabulum, longer pubis and wider GSN. The KNM-ER 3228 reconstructions are close to the pre-Neanderthal cluster in the negative values. They represent a relatively wider ilium with the highest point being in the lateral portion of the coxal bone, as well as bigger and more coronally oriented acetabula, shorter pubis and narrower GSN.

The differences between modern shape and the other three groups are statistically significant ($p < 0.001$). The same goes for the Neanderthal sample (Procrustes distance = 0.128, $p < 0.001$ between Neanderthal and Middle Pleistocene; Procrustes distance = 0.171, $p = 0.009$ between Neanderthal and early *Homo*). Differences between the Middle Pleistocene individuals and early *Homo* are also statistically significant (Procrustes distance = 0.133, $p = 0.029$).

Excluding the early *Homo* reconstructions, body shape is still most represented by PC2 (11.52%). In this analysis, all Neanderthal individuals cluster together, with the SH Pelvis 1 reconstructions being inside the Neanderthal 95% confidence ellipse (Fig. 3), and the Arago XLIV reconstructions remain isolated in the positive values of the PC. The morphological differences explained by the PC2 axis are the same as in the previous analysis for the ilium (wider with a differently positioned highest point) and the position of the acetabulum. But in this case, the size of the acetabulum is similar in both clusters, and now it is the Neanderthal morphology, which exhibits a relatively shorter pubis with a narrower GSN, indicating the mixture of body shape and sexual dimorphism signal on the PCs.

In this case, the differences between modern shape and the other three groups are also statistically significant ($p < 0.001$), and the same goes for the differences between Neanderthal and Middle Pleistocene morphologies (Procrustes distance = 0.128, $p = 0.002$). If the SH Pelvis 1 reconstructions are taken out of the Middle Pleistocene group, based on the PCA results, and a new discriminant analysis is performed, the differences between Neanderthal and Arago (Procrustes distance = 0.155, $p = 0.004$) are significant. The Pelvis 1 morphology is not significantly different from either Neanderthal (Procrustes distance =

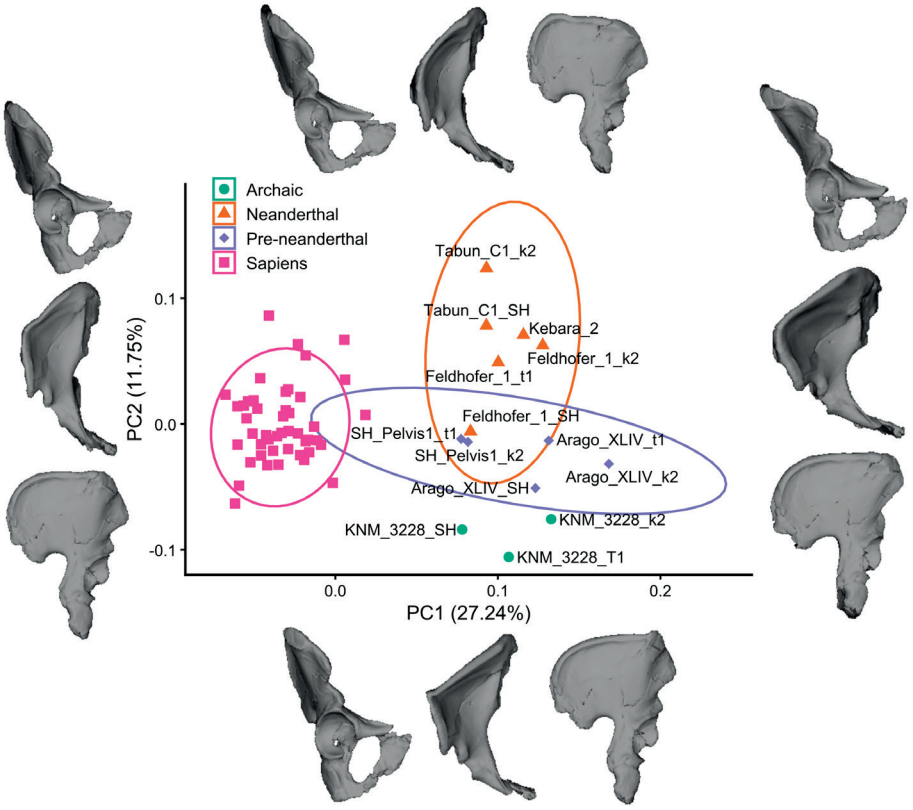

***Fig. 2** – PC1 versus PC2 for the whole sample. Groups are determined by 95% confidence ellipses. The warpings associated with the maximum and minimum PC scores of each PC are shown at the extreme of each axis in lateral, anterolateral, superior, and posterior views.*

0.140, p = 0.070) nor Arago (Procrustes distance = 0.156, p = 0.057) morphologies.

Since the sample of *H. sapiens* is much larger than that of Neanderthal lineage individuals, a second verification analysis was conducted to assess the bias introduced by the sample difference, using only three *H. sapiens* individuals of each sex and the Neanderthal lineage sample. In this new analysis, PCs 1-3 explain 65.16% of the total variability. As in the analysis of the complete sample, PC1 (32.98%) corresponds to the differences between the two groups. PC2 (17.51%) corresponds to differences related to both sexual dimorphism and overall body shape, and PC3 (14.67%) corresponds mostly to differences in sexual dimorphism (Suppl. Mat. Figs. 1 and 2).

Discussion

Geometric morphometrics allows the study of hip bone morphology and the distinction between male and female shapes in anatomically modern individuals (Candelas et al. 2017). This technique has been applied to extinct hominins and modern *H. sapiens* to assess variation related to body shape and sexual dimorphism.

Our results show that there are differences in hip bone morphology between the different body shapes within the *Homo* genus. PC1 positive values (Figs. 2 and 3) show the known *Homo sapiens* coxal bone characteristics in relation to archaic hominins: overall smaller, gracile, with no iliac lateral flaring, a relatively shorter

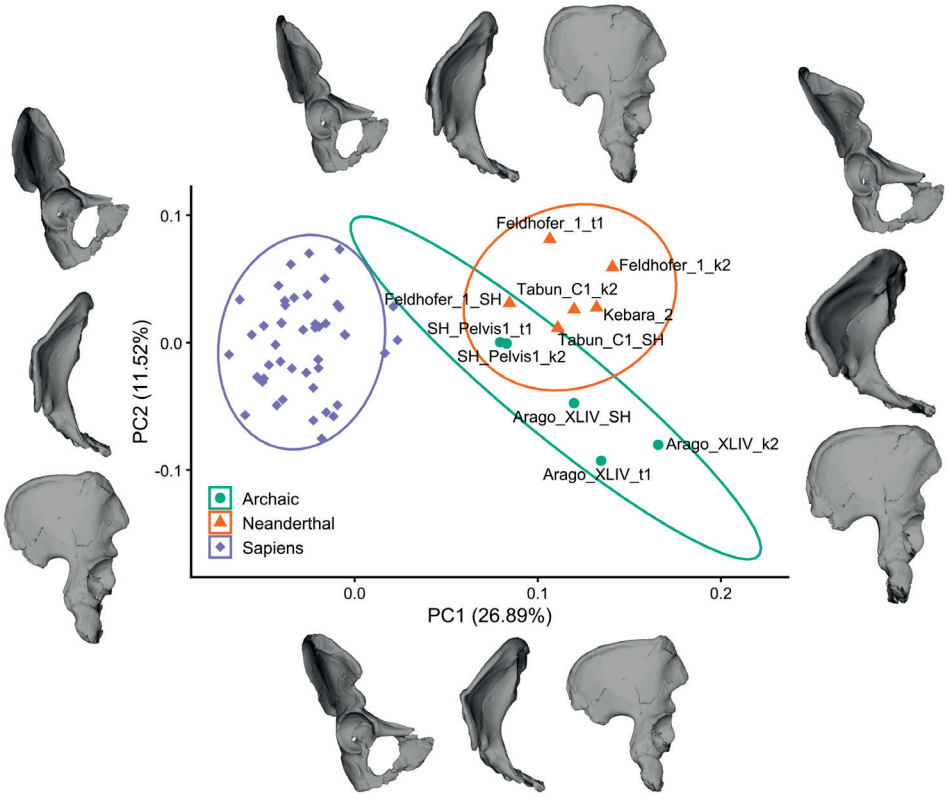

***Fig. 3** – PC1 versus PC2 for the Neanderthal sample. Groups are determined by 95% confidence ellipses. The warpings associated with the maximum and minimum PC scores of each PC are shown at the extreme of each axis in lateral, anterolateral, superior, and posterior views.*

superior pubic ramus and a more coronally positioned acetabulum (Trinkaus 1984; Rak and Arensburg 1987; Rosenberg 1999; Arsuaga et al. 1999; Torres-Tamayo et al. 2025). Meanwhile, both Neanderthal and earlier individuals present more robust coxal bones, with a relatively elongated superior pubic ramus, a laterally positioned acetabulum and marked lateral iliac flaring. This supports the hypothesis that the wider body shape represents the ancestral condition in *Homo* (Carretero et al. 2004).

On the other hand, the whole-sample PC2 (Fig. 2) shows a morphological gradient from a more archaic shape (wider and more laterally flaring iliac blades with a more lateral highest point) to a more Neanderthal-derived morphology (narrower, slightly more vertical and with a medial highest point in the iliac blades), with the three groups (early *Homo*, Middle Pleistocene and Neanderthals) being statistically different from one another. Also, in Fig. 3, SH Pelvis 1 is graphically clustered with the Neanderthal sample, and it is not significantly different from either the Neanderthal or the "Arago XLIV" shapes. These results could imply a gradual evolution in the Neanderthal lineage from the plesiomorphic to the Neanderthal body shape, with the Sima de los Huesos individual being closer to the Neanderthal morphology than Arago XLIV. Our results support the "accretion model" (Dean et al. 1998) of Neanderthal evolution, and also the "phylogeographic evolutionary scenario" (Di Vincenzo and Manzi 2023).

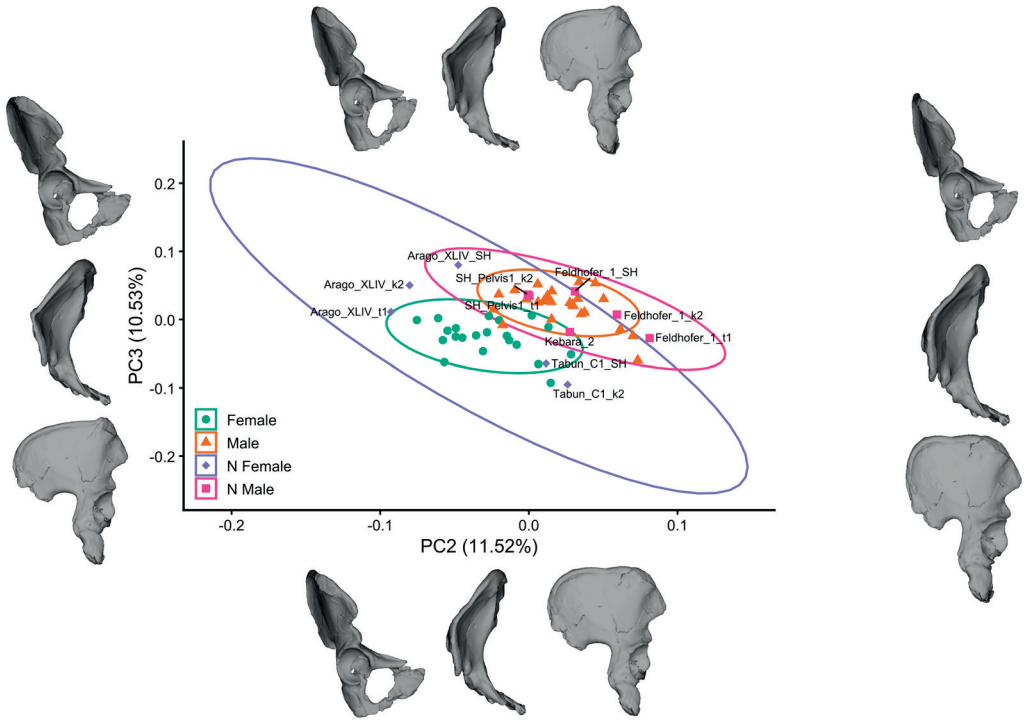

***Fig. 4** – PC2 versus PC3 for the Neanderthal sample. Groups are determined by 95% confidence ellipses. The warpings associated with the maximum and minimum PC scores of each PC are shown at the extreme of each axis in lateral, anterolateral, superior, and posterior views.*

The reconstruction of Feldhofer 1 using SH Pelvis 1 as the reference is the only individual beyond its theoretical range. The original Feldhofer 1 fossil is missing some of the landmarks that determine iliac blade width, maximum height and lateral flaring. Naturally, the reconstruction based on an archaic iliac blade morphology introduces a bias in the classification of the individual, but at the same time it is helpful to understand the key differences between the groups.

The sexual classification obtained through geometric morphometrics matches that reported in the literature for all individuals except for the reconstruction of Arago XLIV based on SH Pelvis 1 (Fig. 4). Originally assessed as a female (de Lumley 2015), a recent study (Rmoutilová et al. 2024) reassessed the sexual determination of Arago XLIV and classified it as female using a visual method (Santos et al. 2019) and as indeterminate (89.9% probability of being male) using a metrical method (DSP2; Bruzek et al. 2017). PC2 and PC3 divide male and female individuals based mainly on pubic length, ilium width, and GSN aperture. Of these main characteristics, the original fossil of Arago XLIV presents a wide ilium and a wide GSN, but the pubis and part of the ischium are not preserved and have been reconstructed using three different references. This reconstruction introduced substantial bias in the analysis, and the three reconstructions are placed on the female or male morphospace depending on the relative pubic length of the reference (Tabun C1 > Kebara 2 > SH Pelvis 1).

This bias can also be seen in the LDA analysis, where the Pelvis 1 reconstruction of Arago XLIV is classified as male while the other two reconstructions are classified as female. This suggests that the methodology used in this study may not be best suited to assess sexual dimorphism in fossils lacking the pubis.

The PCA also shows that all the individuals follow the same distribution pattern along PC2 vs. PC3, regardless of their body shape (Fig. 4). Neanderthal lineage individuals of both body shapes had longer pubic bones than *H. sapiens* (Trinkaus 1984; Rosenberg 1988). This is a plesiomorphic character (Arsuaga et al. 1999; Simpson et al. 2008; Bonmatí et al. 2010) that has also been hypothesized to be the result of an adaptation to cold environments (Weaver and Hublin 2009), different locomotion mechanisms (Weaver et al. 2016) or larger body sizes (Rosenberg 1988). In Neanderthal fossils with preserved pubic bones, those classified as male exhibit a longer superior pubic ramus than female ones (Weaver et al. 2016), but the difference in absolute length is due to the preserved male specimens being significantly larger than the Neanderthal male average, while the female specimens fall within the female average (Rosenberg 1988). The results of this study show that Neanderthal female pubic length is relatively higher than in males, following the same pattern as in *H. sapiens*. Kebara 2 has traditionally been assessed as male (Rak and Arensburg 1987), but its long superior pubic ramus and high ischiopubic index (Arsuaga et al. 1999) make it closer to the female shape in our analyses and may be the reason why the LDA classifies it as female in the *H. sapiens* morphospace.

The Neanderthal lineage individuals share the same range and distribution as the anatomically modern sample, which would imply a similar pattern of sexual dimorphism. However, the results must be taken with caution. The fossil sample is small, so only a small part of the whole Neanderthal and pre-Neanderthal variability is being analysed. Moreover, the fragmented nature of most of the fossil record requires the reconstruction of significant parts of the bones, which introduces bias in the analyses.

Conclusions

Our results point to a similar sexual dimorphism pattern in the coxal bone between the Neanderthal lineage individuals and Homo sapiens *(H1), regardless of body shape (H2), where the female individuals present a relatively longer superior pubic ramus, wider iliac blades, and a wider greater sciatic notch than males. Also, there seems to be a gradient from a primitive morphology present in early Homo to the derived Neanderthal coxal bone morphology, with the Sima de los Huesos individual being more Neanderthal-like than Arago XLIV. This is in line with the accretion and phylogeographic evolutionary hypotheses for Neanderthal evolution.*

Acknowledgements:

The Laboratorio de Poblaciones del Pasado (LAPP) has been supported by Projects PGC2018-099405-B-100, HAR2017-82755-P, HAR2017-83004-P, HAR2016-78036-P, HAR2016-74846-P (Spanish Government), a grant (ref. 38360) from The Leakey Foundation and Comunidad de Madrid (ref. SI4/PJI/2024-00104). Grant PID2020-115854GB-I00 to MB is funded by MCIN/AEI/10.13039/501100011033 of the Spanish Ministry of Science and Innovation and the European Union. Grant PIPF-2024/SAL-GL-34325 to GML by Community of Madrid through the Predoctoral Research Staff Training Program (PIPF). We thank Alon Barash for giving access to the Kebara 2 3D model, Carmen Cacho and Eduardo Galán from the Prehistory department of Museo Arqueológico Nacional of Madrid for allowing the 3D scan of SH Pelvis 1, Aidan Paul and the RLA Archaeology group from the University of North Carolina for the open access of the Neanderthal 1 3D model at Sketchfab, and The Natural History Museum of London for access to the Tabun C1 reconstruction. We thank the National Museums of Kenya, E. Mbua and F. Kyalo Manthi for permissions to scan KNM-ER 3228 and the Arago XLIV cast.

Declaration of interest statement

There is no conflict of interest

Orcid IDs

Gonzalo Madroñal López:
https://orcid.org/0009-0009-6961-838X
Nieves Candelas González:
https://orcid.org/0000-0001-9978-5407
Armando González Martín:
https://orcid.org/0000-0001-9216-1220
Markus Bastir:
https://orcid.org/0000-0002-3141-3401
Daniel García-Martínez:
https://orcid.org/0000-0001-7518-3866

References:

Adams D, Collyer M, Kaliontzopoulou A, et al (2025) Geomorph: Software for geometric morphometric analyses. R package version 4.0.10. https://cran.r-project.org/package=geomorph

Arsuaga JL, Lorenzo C, Carretero JM, et al (1999) A complete human pelvis from the Middle Pleistocene of Spain. Nature 399:255-258. https://doi.org/10.1038/20430

Auerbach BM, King KA, Campbell RM, et al (2018) Variation in obstetric dimensions of the human bony pelvis in relation to age-at-death and latitude. Am J Phys Anthropol 167:628-643. https://doi.org/10.1002/ajpa.23690

Baab KL, McNulty KP, Rohlf FJ (2012) The Shape of Human Evolution: A Geometric Morphometrics Perspective. Evol Anthropol 21:151-165. https://doi.org/10.1002/evan.21320

Baken E, Collyer M, Kaliontzopoulou A, et al (2021) geomorph v4.0 and gmShiny: enhanced analytics and a new graphical interface for a comprehensive morphometric experience. Methods Ecol. Evol. 12:2355-2363. https://doi.org/10.1111/2041-210X.13723

Bastir M, García-Martínez D, Torres-Tamayo, N, et al (2019) Workflows in a Virtual Morphology Lab: 3D scanning, measuring, and printing. JASs 97:1-28. https://doi.org/10.4436/jass.97003

Been E, Gómez-Olivencia A, Shefi S, et al (2017) Evolution of Spinopelvic Alignment in Hominins. Anat Rec 300:900-911. https://doi.org/10.1002/ar.23559

Betti L, von Cramon-Taubadel N, Manica A, et al (2013) Global Geometric Morphometric Analyses of the Human Pelvis Reveal Substantial Neutral Population History Effects, Even across Sexes. PLoS One 8:e55909. https://doi.org/10.1371/journal.pone.0055909

Betti L (2014) Sexual Dimorphism in the Size and Shape of the Os Coxae and the Effects of Microevolutionary Processes. Am J Phys Anthropol 153:167-177. https://doi.org/10.1002/ajpa.22410

Bonmatí A, Gómez-Olivencia A, Arsuaga JL, et al (2010) Middle Pleistocene lower back and pelvis from an aged human individual from the Sima de los Huesos site, Spain. Proc Natl Acad Sci USA 107:18386-18391. https://doi.org/10.1073/pnas.1012131107

Bookstein FL (1991) Morphometric Tools for Landmark Data: Geometry and Biology. University Press, Cambridge. https://doi.org/10.1017/CBO9780511573064

Bruzek J, Murail P (2006) Methodology and reliability of sex determination from the skeleton. In: Schmitt A, Cunha E, Pinheiro J (eds) Forensic Anthropology and Medicine. Complementary sciences from recovery to cause of death, Humana Press, New Jersey, p. 225-242. https://doi.org/10.1007/978-1-59745-099-7_9

Bruzek J, Santos F, Dutailly B, et al (2017) Validation and reliability of the sex estimation of the human *os coxae* using freely available DSP2 software for bioarchaeology and forensic anthropology. Am J Phys Anthropol 164:440-449. https://doi.org/10.1002/ajpa.23282

Bytheway JA, Ross AH (2010) A Geometric Morphometric Approach to Sex Determination of the Human Adult Os Coxa. J Forensic Sci 55:859-864. https://doi.org/10.1111/j.1556-4029.2010.01374.x

Candelas González N, Rascón Pérez J, Chamero B, et al (2017) Geometric morphometrics

reveals restrictions on the shape of the female *os coxae*. J Anat 230:66-74. https://doi.org/10.1111/joa.12528

Carretero JM, Arsuaga JL, Martínez J, et al (2004) Los humanos de la Sima de los Huesos (Sierra de Atapuerca) y la evolución del cuerpo en el género *Homo*. In: Baquedano E, Rubio Jara S (coords) Homenaje a Emiliano Aguirre, Vol. 4, Museo Arqueológico Regional, Madrid, p. 120-136.

De Lumley MA (2015) L'homme de Tautavel. Un *Homo erectus* européen évolué. *Homo erectus tautavelensis*. L'Anthropologie 119:303-348. https://doi.org/10.1016/j.anthro.2015.06.001

Dean D, Hublin JJ, Holloway R, et al (1998) On the phylogenetic position of the pre-Neandertal specimen from Reilingen, Germany. J Hum Evol 34:485-508. https://doi.org/10.1006/jhev.1998.0214

Di Vincenzo F, Manzi G (2023) *Homo heidelbergensis* as the Middle Pleistocene common ancestor of Denisovans, Neanderthals and modern humans. JMES 15:303-315. https://doi.org/10.13133/2280-6148/18074

EVAN-Society (2010) EVAN Toolbox (Version 1.75). European Virtual Anthropology Network. Available at: https://www.evan-society.org/support/download-evan-toolbox/

Ferembach D, Schwidetzky I, Stloukal M (1980) Recommendations for age and sex diagnoses of skeletons. J Hum Evol 9:517-549. https://doi.org/10.1016/j.jchb.2005.07.002

Fischer B, Grunstra NDS, Zaffarini E, et al (2021) Sex differences in the pelvis did not evolve de novo in modern humans. Nat Ecol Evol 5:625-630. https://doi.org/10.1038/s41559-021-01425-z

Franciscus RG (2009) When did the modern human pattern of childbirth arise? New insights from an old Neanderthal pelvis. Proc Natl Acad Sci USA 106:9125-9126. https://doi.org/10.1073/pnas.0903384106

Gunz P, Mitteroecker P, Neubauer S, et al (2009) Principles for the virtual reconstruction of hominin crania. J Hum Evol 57:48-62. https://doi.org/10.1016/j.jhevol.2009.04.004

Haeusler M, Grunstra NDS, Martin RD, et al (2021) The obstetrical dilemma hypothesis: there's life in the old dog yet. Biol Rev 96:2031-2057. https://doi.org/10.1111/brv.12744

Holliday TW (2012) Body Size, Body Shape, and the Circumscription of the Genus *Homo*. Current Anthropology 53:330-345. https://doi.org/10.1086/667360

Klales AR (2020) Sex estimation using pelvis morphology. In: Klales AR (ed) Sex Estimation of the Human Skeleton, Academic Press, London, p. 75-93. https://doi.org/10.1016/B978-0-12-815767-1.00006-7

Klingenberg CP (2011) MorphoJ: an integrated software package for geometric morphometrics. Mol Ecol Resour 11:353-357. https://doi.org/10.1111/j.1755-0998.2010.02924.x

Leakey REF (1976) New hominid fossil from the Koobi For a formation in Northern Kenya. Nature 261:574-576. https://doi.org/10.1038/261574a0

López-Rey JM, García-Martínez D, Bastir M (2025) Shanidar 3 'rings the bell': Virtual ribcage reconstruction and its implications for understanding the Neanderthal bauplan. J Hum Evol 199:103629. https://doi.org/10.1016/j.jhevol.2024.103629

Lycett SJ, von Cramon-Taubadel N (2013) Understanding the comparative catarrhine context of human pelvic form: A 3D geometric morphometric analysis. J Hum Evol 64:300-310. http://dx.doi.org/10.1016/j.jhevol.2013.01.011

McCown TD, Keith A (1939) The Stone Age of Mount Carmel II: The Fossil Human Remains from the Levalloiso-Mousterian, Clarendon Press, Oxford. https://doi.org/10.1017/S0079497X00020491

Murail P, Bruzek J, Houët F, et al (2005) DSP: A tool for probabilistic sex diagnosis using worldwide variability in hip-bone measurements. Bull Mém Soc Anthropol Paris n.s. 17:167-176. https://doi.org/10.4000/bmsap.1157

Ponce de León MS, Golovanova L, Doronichev V, et al (2008) Neanderthal brain size at birth provides insight into the evolution of human life history. Proc Natl Acad Sci USA 105:13764-13768. https://doi.org/10.1073/pnas.0803917105

R Core Team (2025) R: A Language and Environment for Statistical Computing. R Foundation for Statistical Computing. https://www.r-project.org/

Rak Y, Arensburg B (1987) Kebara 2 Neanderthal pelvis: first look at a complete inlet. Am J Phys Anthropol 73:227-231. https://doi.org/10.1002/ajpa.1330730209

Rascón Pérez J (2017) Análisis de las diferencias sexuales en la morfología del esqueleto y de la distribución de caracteres de interés relacionados con el sexo. Estudio de dos series medievales de la Península Ibérica, Doctoral dissertation, Universidad Autónoma de Madrid. https://repositorio.uam.es/handle/10486/680138?show=full

Rissech C, Sañudo JR, Malgosa A (2001) The acetabular point: a morphological and ontogenetic study. J Anat 198:743-748. https://doi.org/10.1046/j.1469-7580.2001.19860743.x

Rmoutilová R, Bruzek J, Gómez-Olivencia A, et al (2024) Sex estimation of the adult Neandertal Regourdou 1 (Montignac, France): Implications for sexing human fossil remains. J Hum Evol 189:103470. https://doi.org/10.1016/j.jhevol.2023.103470

Robertson HI, Pokotylo DL, Weston DA (2019) Testing landmark redundancy for sex-based shape analysis of the adult human os coxa. Am J Phys Anthropol 169:689-703. https://doi.org/10.1002/ajpa.23860

Rosenberg KR (1988) The functional significance of neandertal pubic length. Curr Anthropol 29:595-617. https://doi.org/10.1086/203678

Rosenberg KR (1992) The evolution of modern human childbirth. Yearb Phys Anthropol 124:35-89. https://doi.org/10.1002/ajpa.1330350605

Ruff CB (1995) Biomechanics of the hip and birth in Early *Homo*. Am J Phys Anthropol 98:527-574. https://doi.org/10.1002/ajpa.1330980412

Ruff CB (2002) Variation in human body size and shape. Annu Rev Anthropol 31:211-232. https://doi.org/10.1146/annurev.anthro.31.040402.085407

Ruff CB (2010) Body size and body shape in early hominins – implications of the Gona Pelvis. J Hum Evol 58:166-178. https://doi.org/10.1016/j.jhevol.2009.10.003

Santos F, Guyomarc'h P, Rmoutilová R, et al (2019) A method of sexing the human os coxae based on logistic regressions and Bruzek's nonmetric traits. Am J Phys Anthropol 169:435-447. https://doi.org/10.1002/ajpa.23855

Schaaffhausen H (1888) Der Neanderthaler-Fund. Marcus, Bonn, Germany.

Schlager S (2017) Morpho and Rvcg – Shape Analysis in R. In: Zheng G, Li S, Szekely G (eds) Statistical shape and deformation analysis, Academic Press, London, p. 217–256. https://doi.org/10.1016/B978-0-12-810493-4.00011-0

Simpson S, Quade J, Levin NE, et al (2008) A female *Homo erectus* pelvis from Gona, Ethiopia. Science 322:1089-1092. https://doi.org/10.1126/science.1163592

Skoglund P, Storå J, Götherström A, et al (2013) Accurate sex identification of ancient human remains using DNA shotgun sequencing. J Archaeol Sci 40:4477-4482. https://doi.org/10.1016/j.jas.2013.07.004

Stansfield E, Kumar K, Mitteroecker P, et al (2021) Biomechanical trade-offs in the pelvic floor constrain the evolution of the human birth canal. Proc Natl Acad Sci USA 118:e2022159118. https://doi.org/10.1073/pnas.2022159118

Stanyon R, Consigliere S, Morescalchi MA (1993) Cranial Capacity in Hominid Evolution. Hum Evol 8:205-216. https://doi.org/10.1007/BF02436715

Trinkaus E (1984) Neandertal pubic morphology and gestation length. Curr Anthropol 25:509–514. https://doi.org/10.1086/203173

Venables WN, Ripley BD (2002) Modern Applied Statistics with S, fourth edition, Springer, New York. https://www.stats.ox.ac.uk/pub/MASS4/

Washburn SL (1960) Tools and Human Evolution. Sci Am 203:63-75. https://doi.org/10.1038/SCIENTIFICAMERICAN0960-62

Weaver TD, Coqueugniot H, Golovanova LV, et al (2016) Neonatal postcrania from Mezmaiskaya, Russia, and Le Moustier, France, and the developement of Neandertal body form. Proc Natl Acad Sci USA

113:6472-6477. https://doi.org/10.1073/pnas.1523677113

Weaver TD, Hublin JJ (2009) Neandertal birth canal shape and the evolution of human childbirth. Proc Natl Acad Sci USA 106:8151-8156. https://doi.org/10.1073/pnas.0812554106

Wickham H (2016) ggplot2: elegant graphics for data analysis, Springer-Verlag, New York. https://ggplot2.tidyverse.org/

Zelditch ML, Swiderski DL, Sheets HD (2012) Basics of Shape Data. In: Zelditch ML, Swiderski DL, Sheets HD (eds) Geometric Morphometrics for Biologists: A Primer, Second Edition. Elsevier, London, p. 23-103.

Associate Editor, Fabio Di Vincenzo

This work is distributed under the terms of a Creative Commons Attribution-NonCommercial 4.0 Unported License http://creativecommons.org/licenses/by-nc/4.0/